Zeitschrift: IABSE reports of the working commissions = Rapports des commissions de travail AIPC = IVBH Berichte der Arbeitskommissionen

Band: 19 (1974)

Artikel: Analysis of podded boiler type PCPV with reference to the analysis of solid of revolution

Autor: Kawamata, S.

DOI: https://doi.org/10.5169/seals-17520

IABSE
AIPC
IVBH

SEMINAR on:
« CONCRETE STRUCTURES SUBJECTED TO TRIAXIAL STRESSES »
17th - 19th MAY, 1974 - ISMES - BERGAMO (ITALY)

Analysis of Podded Boiler Type PCPV with Reference to the Analysis of Solid of Revolution

Analyse d'un caisson en béton précontraint du type «Podded Boiler» avec référence à l'analyse d'un solide de révolution

Die Berechnung eines «Podded Boiler Type PCPV» als Umdrehungs Körper

S. KAWAMATA
Associate Professor, Institute of Industrial Science
University of Tokyo, Tokyo, Japan

SUMMARY

Simplified finite element three-dimensional elastic analysis of the podded boiler type PCPV is discussed.

The first part deals with consistent method of assessing the effective rigidity of standpipe zone, where finite element analyses of the unit area of regular hole pattern are utilized.

In the second part "method of sliced substructures", a new method of simplified three-dimensional analysis of PCPV is proposed. The stiffness of PCPV is evaluated as the combination of stiffness matrix of modified axi-symmetric problems and two-dimensional stiffness matrices of horizontally sliced substructures. This method enables us to analyze the three-dimensional problems of PCPV allowing for the effect of boiler pods within the same degrees of freedom as the axi-symmetric analysis.

The validity of the new method is shown by numerical examples.

1. INTRODUCTION

The finite element method has been widely accepted in the structural analysis for the design of PCPV because of its efficiency, accuracy and adaptability to the general purpose programs. Starting from elastic analysis, the scope of the finite element analysis in the PCPV design has been broadened to wider fields of heat conduction problem, time dependent creep problem, tracing of cracking and failure process, etc.

For the design of PCPV of the gas-cooled reactors and the advanced gas-cooled reactors, the finite element analysis in the form of axi-symmetric problems of body of revolution was efficiently adapted, resulting high accuracy with small degrees of two-dimensional freedom.

However, as discussed in the review by Argyris et.al.[1], having various kinds of openings such as standpipe zone in the top slab and coolant circulator deposits, stress in PCPV has some discrepancies from the axi-symmetric condition.

The effect of the multiple perforations of standpipe zone has been taken into account by simply reducing the elastic constant within the framework of the axi-symmetric analysis [2,3,4]. But the consideration of the stress disturbance induced by major openings gives rise to necessity of three-dimensional analysis [5].

In the early stage, the three-dimensional finite element analysis, having very large degrees of freedom and band width of the system stiffness matrices, required huge amount of memory, computing time, labour for input data preparation and consequently high cost of analysis. The development of the iso-parametric element technique [6] put the cost of the three-dimensional elastic analysis of PCPV in the range of reasonable investment for the design purpose [1,7].

The geometry of the podded boiler type PCPV recently developed for AGR and HTGR, having vertical cavities within the thickness of vessel wall, leads to the indispensable practice of the three-dimensional analysis for each phase of design, i.e. elastic, time-dependent and failure analyses. Even the most efficient program of three-dimensional elastic analysis seems to require more than ten times of computation time compared with the corresponding axi-symmetric analysis of the same accuracy. Even if this situation is acceptable for the elastic analysis, the cost of three-dimensional creep and failure analyses, which involve numerous repetition of stress redistribution process, will amount to unrealistic one as a tool for the structural design. Lewis et.al.[4] discussed this problem and suggested the use of simply rough mesh of element idealization. But rather poor representation of strain distribution shown in his example cautions us to the possibility of getting inaccurate results which will be caused by the errors accumulated in the course of repeated steps.

Thus, when considering the step analyses for the long-term and failure situation, the type of finite element three-dimensional treatment must be determined on the balance between the cost and labour of computation and the accuracy of the results obtainable at these expense. In this sense, more efficient scheme of the three-dimensional finite element elastic analysis of PCPV, which can provide

the acceptable accuracy within computing time not much exceeding the one required for the axi-symmetric problems, is worth searching.

The object of this paper is to present a new scheme of simplified finite element three-dimensional elastic analysis of the podded boiler type PCPV, in which a modified axi-symmetric treatment of solids of revolution combined with condensed stiffness matrices of two-dimensional "sliced substructures" is utilized.

The first part of the paper describes the transformation of the standpipe zone of top slab into an equivalent homogeneous transversely isotropic medium which enables more consistent treatment of axi-symmetric analysis than in the case of simple reduction of Young's modulus done in the previous practices [4]. By the two-dimensional finite element analyses of the unit area formed by the regular patterns of perforations, each of the elastic constants of the equivalent transversely isotropic body is assessed. The same type of the unit zone analysis was done by Meijers [8,9]. The present method has been developed by the author with collaborators since 1967 [10]. It includes the evaluation of the equivalent transverse shear modulus and constitutes an important part of the new method of modified axi-symmetric analysis.

The latter half of the paper devoted to the description of "method of sliced substructures". In the method of sliced substructures, the three-dimensional portion to be analysed is divided into a number of horizontally sliced layers which have the shape of partial rings having a circular opening of the boiler pod in them.

A dual system of assumed displacement field is adopted. For the system of the structural resistance in the direction of the vertical z-axis and the shearing resistance of the vertical r-z plane, the well known displacement mode of axi-symmetric problems is assumed, i.e. two-dimensional displacements u and w which are constant along the circumference are taken. Similarly to the axi-symmetric case, the stiffness based on this system of resistance is evaluated with regard to the nodal points in the vertical plane of symmetry with regard to the specified resistance.

On the other hand, the resistance formed by the strain in horizontal plane is evaluated separately for each layer of the horizontal slices; each slice is devided into a two-dimensional finite element mesh in r-θ plane and the stiffness matrix for the total slice area is formed as the ordinary plane stress problem. Then the unknown displacements of the interior part of the slice are eliminated by the static condensation, only the nodal displacements in the radial direction u on the plane of symmetry being retained as unknowns. The displacement assumed for this system of horizontal resistance has two-dimensional freedom in r-θ plane but is constant within the thickness of the slice.

Both stiffness matrices, one representing axial and shearing resistance and the other the resistance in the horizontal plane, are combined on the vertical section of symmetry, taking the nodal displacements u in the both system as the same unknown. This means the final system equation has the same degrees of freedom as the

axi-symmetric problems, i.e. twice the number of nodes in the vertical section of symmetry.

In this scheme, dual mode of the displacement is assumed, namely different assumptions of displacements are adopted for the two groups of stresses.

Therefore, the present method can be interpreted as a kind of the method of partial approximation, which has lately been investigated by Kikuchi in the field of finite element shell analysis [11-13]. The assumed horizontal displacement fields in the sliced substructures contain incompatibility in the boundary surfaces between upper and lower layers, and the convergence criteria is not yet clear for the present scheme of approximation. Therefore, the validity and the efficiency of the method must be investigated by numerical experiments on the actual problems of podded boiler PCPV.

2. EFFECTIVE ELASTIC COEFFICIENTS OF STANDPIPE ZONE

A method of evaluating the effective elastic constants of the homogeneous medium equivalent to the standpipe zone of triangular hole pattern is described here. Because of the regular pattern of hole arrangement the effective rigidity in respective directions can be assessed by finite element two-dimensional analysis of the constituent unit area of the zone.

Transformed homogeneous body is in general anisotropic. As the cylindrical openings have the axis in the vertical z-direction, it is clear that the equivalent continuum has the different elastic coefficients in z-direction and in r-θ plane. In the r-θ plane, it will have anisotropy of different kind according to the hole pattern. When applying the three-dimensional finite elements for this zone in the analysis of the total vessel, any kind of orthotropy can be assigned to this part. But in order to apply the axi-symmetric analysis for the vessel, transformation into an equivalent transversely isotropic body is required and the averaging of the coefficients is neccessary, when they have different values in different directions.

Fortunately, a triangular hole pattern, having three equiangular lines of symmetry, necessarily leads to isotropy in the horizontal plane, resulting the unique solution of equivalence for the transformed transversely isotropic body. This condition of the triangular pattern allows us to obtain all the elastic coefficients by analyzing the single unit area.

The elastic coefficients for the transversely isotropic body contain 5 parameters and can be given in the following form [14-16].

$$\begin{Bmatrix} \sigma_x \\ \sigma_y \\ \sigma_z \\ \tau_{yz} \\ \tau_{xz} \\ \tau_{xy} \end{Bmatrix} = \begin{bmatrix} d_1 & & & & & \\ d_2 & d_1 & & & \text{symmetry} & \\ d_3 & d_3 & d_4 & & & \\ & & & d_5 & & \\ & & & & d_5 & \\ & & & & & (d_1-d_2)/2 \end{bmatrix} \begin{Bmatrix} \varepsilon_x \\ \varepsilon_y \\ \varepsilon_z \\ \gamma_{yz} \\ \gamma_{xz} \\ \gamma_{xy} \end{Bmatrix} \tag{1}$$

In contrast, in the case of isotropy, we have two-parameter coefficients as

$$\begin{Bmatrix}\sigma_x\\ \sigma_y\\ \sigma_z\\ \tau_{yz}\\ \tau_{xz}\\ \tau_{xy}\end{Bmatrix} = \begin{bmatrix} d_1^0 & & & & & \\ d_2^0 & d_1^0 & & \text{symmetry} & & \\ d_2^0 & d_2^0 & d_1^0 & & & \\ & & & (d_1^0-d_2^0)/2 & & \\ & & & & (d_1^0-d_2^0)/2 & \\ & & & & & (d_1^0-d_2^0)/2 \end{bmatrix} \begin{Bmatrix}\varepsilon_x\\ \varepsilon_y\\ \varepsilon_z\\ \gamma_{yz}\\ \gamma_{xz}\\ \gamma_{xy}\end{Bmatrix} \qquad (2\text{-a})$$

where

$$d_1^0 = \frac{(1-\nu)\,E}{(1+\nu)(1-2\nu)}, \qquad d_2^0 = \frac{\nu\,E}{(1+\nu)(1-2\nu)} \qquad (2\text{-b})$$

Let the perforated zone of top slab shown in Fig.1(a) be considered. The hole pattern shown in Fig.1(b) is assumed to be infinitively spread in the x-y plane and the shaded unit area is to be analyzed. The depth of the slab is assumed also to be infinitive in z-direction.

In order to give the infinitive medium the unit strain in the sense of mean value, relative displacements are subjected between a paticular pair of opposite edges of the unit area, while the boundary faces being kept plane because of the conditions of symmetry. The mean stress evaluated from the boundary face reactions yields the neccesary effective coefficients of elasticity.

1) d_4 : Effective Elastic Coefficient for Normal Stress in z-direction

The effective coefficient d_4 for σ_z can be evaluated, in principle, from the resultant reaction R_z which is caused by prescribing vertical displacement $\delta_z = h$ to the top surface as shown in Fig.2(a).

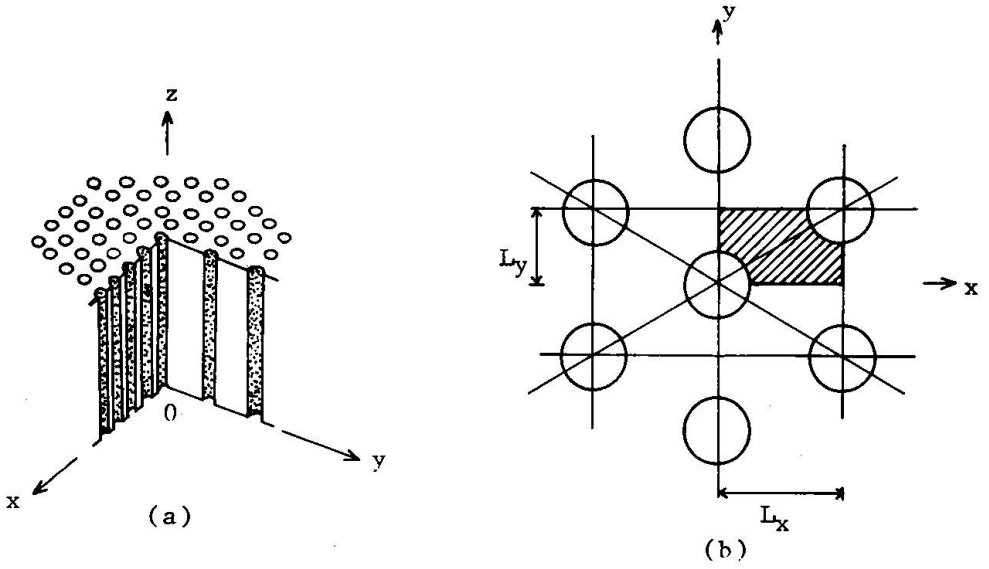

Fig.1 Standpipe Zone and its Hole Pattern

While, this state of stress can be realized also by giving the same displacement to the body, in which the surfaces of the cylindrical holes are constained by rollers, the constraint forces subsequently being released as shown in Fig.2(b). The latter release of constraint will not cause any significant reaction in z-direction when the hole is not very large. Therefore the effective coefficient can be approximately represented by

$$d_4 = \alpha\, d_1^{\circ} \qquad (3\text{-a})$$

where d_1° : coefficient for isotropic case given in Eq.(2-b)

$$\alpha = A/A_o : \qquad (3\text{-b})$$

ratio of perforated to unperforated areas shown in Fig.2(c)

2) d_1, d_2, d_3, : Effictive Elastic Coefficient Derived from Strain in the Plane of Slab

When we put $\varepsilon_x = 1$ in Eq.(1), we have

$$\begin{Bmatrix} \sigma x \\ \sigma y \\ \sigma z \end{Bmatrix} = \begin{Bmatrix} d_1 \\ d_2 \\ d_3 \end{Bmatrix} \qquad (4)$$

Therefore, prescribing displacement $\delta_x = L_x$ as shown in Fig.3, these coefficients can be determined as the mean intensities of the reactions in three directions, i.e.

$$\begin{aligned} d_1 &= \bar{\sigma}_x = R_x/L_y h \\ d_2 &= \bar{\sigma}_y = R_y/L_x h \\ d_3 &= \bar{\sigma}_z = R_z/L_x L_y \end{aligned} \qquad (5)$$

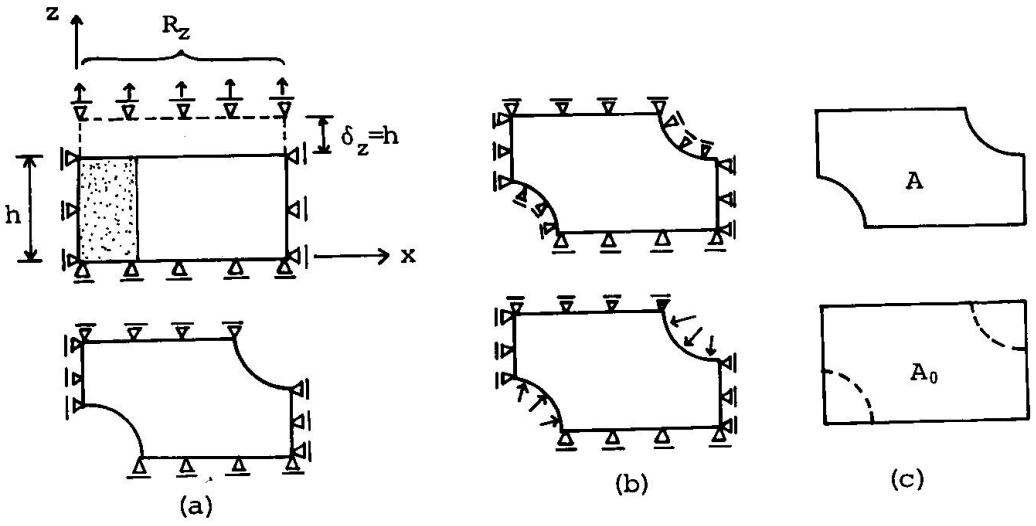

Fig.2 Assessment of Diagonal Coefficient for z-Direction

Besides this, giving $\varepsilon_y = 1$ in the same manner, we have another relation as

$$\begin{Bmatrix} \sigma x \\ \sigma y \\ \sigma z \end{Bmatrix} = \begin{Bmatrix} d_2 \\ d_1 \\ d_3 \end{Bmatrix} \qquad (6)$$

But the coefficients become equal to the ones obtained by the above analysis as the result of the reciprocal theorem.

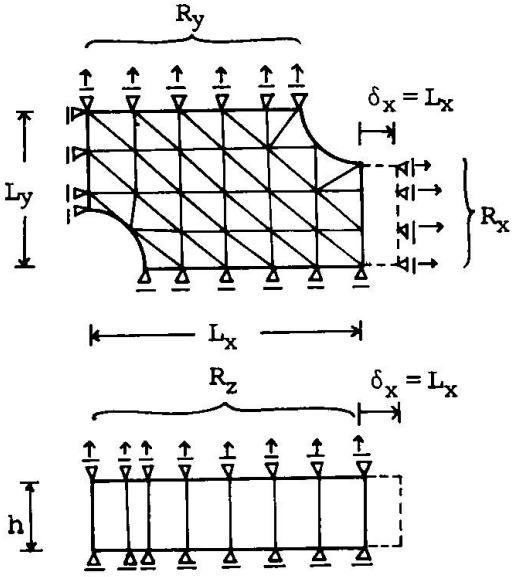

Fig.3 Assessment of Elastic Coefficients d_1, d_2 and d_3

3) d_5 : Coefficient for Transverse Shear

In the infinitive perforated body, an uniform (mean) shearing strain $\bar{\gamma}_{xz}$ is to be prescribed as indicated by Fig.4(a). In order to realize this state, we prescribe $\delta_z = \pm L_x/2$ at the both ends of the solid unit as shown in Fig.4 (b) and (c).

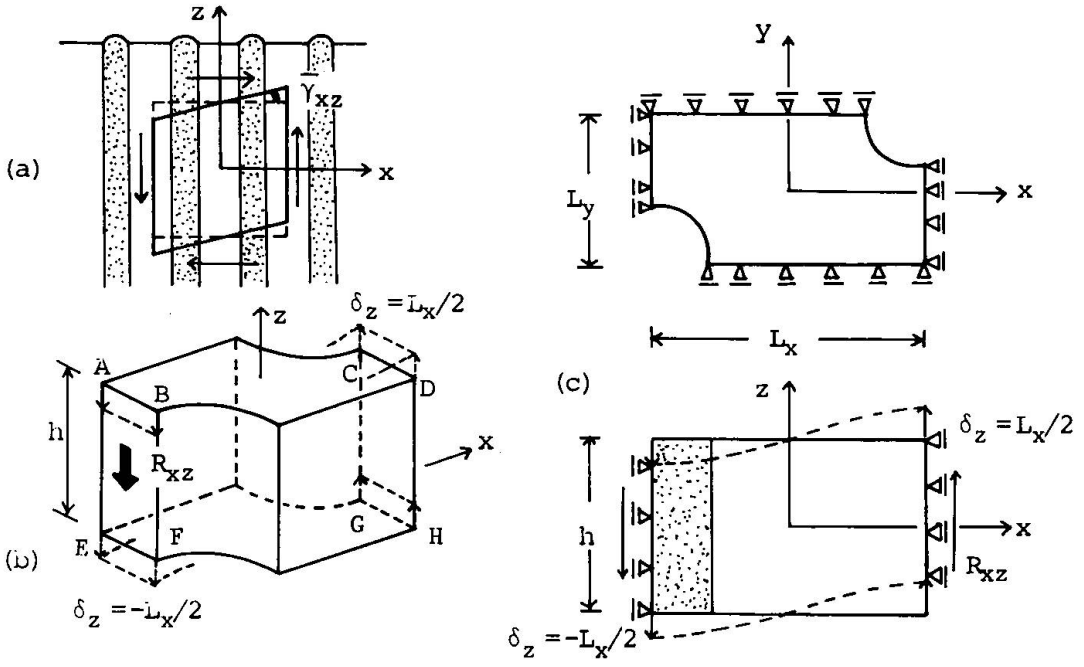

Fig.4 Assessment of Transverse Shear Coefficient, d_5

The resultant vertical force R_{xz} divided gross area of the vertical end face corresponds to the mean shearing stress $\bar{\tau}_{xz}$, leading to the following result :

$$\bar{\tau}_{xz} = \frac{R_{xz}}{L_y h} = d_5 \qquad (7)$$

Though the actual analysis of the solid unit must be carried out by the use of three-dimensional elements, there is no variation of variables in the direction of z-axis from the condition of uniform strain.

Thus, applying the condition of

$$u = u(x,y), \quad v = v(x,y), \quad w = w(x,y) \qquad (8)$$

to the three dimensional nodal displacements, the problem is reduced to two-dimensional one with the stiffness matrix being condensed.

Example of Analysis of Effective Elastic Coefficients

As an example, the effective coefficients for standpipe zone of triangular pattern having the dimensions of

$$\left.\begin{aligned} &L_x = 83\text{cm}, \quad L_y = 48\text{cm} \\ &D = 60\text{cm (diameter of holes)} \end{aligned}\right\} \qquad (9)$$

were analysed. The original moduli of elasticity of the concrete were assumed as

$$E = 3.52 \times 10^6 \text{ kg/cm}^2, \quad \nu = 0.17 \qquad (10)$$

The ratio of perforated to unperforated areas for this example is

$$\alpha = A/A_o = A/L_x L_y = 0.645 \qquad (11)$$

From Eqs.(3) and (11) we obtain

$$d_4 = \alpha d_1' = 0.645 \cdot \frac{(1-\nu)\, E}{(1+\nu)(1-2\nu)} \qquad (12)$$

For obtaining the coefficients d_1, d_2, and d_3, the finite element model shown in Fig.5(a) was analyzed in plane strain state. Prescribed displacements of $\delta_x = L_x$ caused the boundary reactions shown in Figs.5(b) and (c). Vertical reaction resultant R_z was obtained from σ_z in each element using the ralation of

$$\sigma_z = \nu (\sigma_x + \sigma_y) \qquad (13)$$

in the plane strain problem. The final results were calculated as follows :

$$d_1 = \frac{R_x}{L_y h} = \frac{7.23 \times 10^6 \text{kg}}{48.0\text{cm} \times 1\text{cm}} = 1.50 \times 10^5 \text{kg/cm}^2 \qquad (14\text{-a})$$

$$d_2 = \frac{R_y}{L_x\, h} = \frac{3.65 \times 10^6 \text{kg}}{83.0\text{cm} \times 1\text{cm}} = 0.440 \times 10^5 \text{kg/cm}^2 \qquad (14\text{-b})$$

$$d_3 = \frac{R_z}{L_x L_y} = \frac{131.2 \times 10^6 \text{kg}}{48.0\text{cm} \times 83.0\text{cm}} = 0.329 \times 10^5 \text{kg/cm}^2 \qquad (14\text{-c})$$

The reduction of the elastic coefficient from the original solid caused by the perforations can be represented by the following relations :

$$\left.\begin{aligned} d_1 &= 0.396 \times d_1^0 = 0.396 \times \frac{(1-\nu)\,E}{(1+\nu)(1-2\nu)} \\ d_2 &= 0.568 \times d_2^0 = 0.568 \times \frac{\nu E}{(1+\nu)(1-2\nu)} \\ d_3 &= 0.579 \times d_3^0 = 0.579 \times \frac{\nu E}{(1+\nu)(1-2\nu)} \end{aligned}\right\} \qquad (15)$$

The equivalent Young's modulas and Poisson's ratio in x-y plane are correlated to those of the original solid as

$$\left.\begin{aligned} E_1 &= 0.37\, E \\ \nu_1 &= 1.34\, \nu \end{aligned}\right\} \qquad (16)$$

For the analysis of the transverse shear coefficient d_5, a finite element mesh shown in Fig.6(a) was used, where the iso-parametric solid elements of 20 nodes were incorpotated. Prescribing $\delta_z = \pm 1/2\text{cm}$ on both end faces, the nodal vertical reactions shown in Fig.6(d) were obtained. From the resultant $\bar{R}_{xz}$ of these reactions, the shear coefficient was obtained as

$$d_5 = \frac{R_{xz}}{L_y\, h} = \frac{\bar{R}_{xy} L_x}{L_y\, h} = \frac{22.63 \times 10^6 \text{kg/cm} \times 83.0\text{cm}}{48.0\text{cm} \times 564\text{cm}}$$

$$= 0.0694 \times 10^6 \text{kg/cm}^2 \qquad (17)$$

The reduction of the shear coefficient is indicated by the relation

$$d_5 = 0.461\, G \qquad (18)$$

where

$$G = E/2(1+\nu) = (d_1^0 - d_2^0)/2 \;:$$

shear modulas of the unperforated solid

The distribution of the vertical displacement is shown in Fig.6 (b). Fig.6(c) shows the resultant vectors of shear stress component τ_{xz} and τ_{yz} together with its intensity represented by the factor to the mean shearing stress $\bar{\tau}_{xz}$.

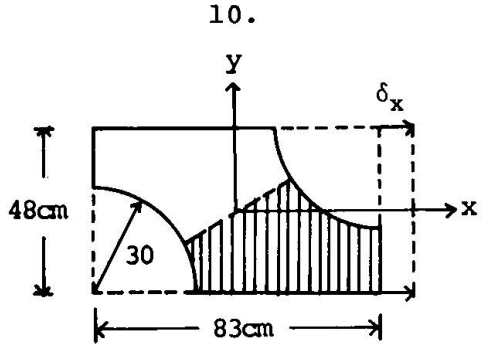

108 elements
73 nodes
for tot. area

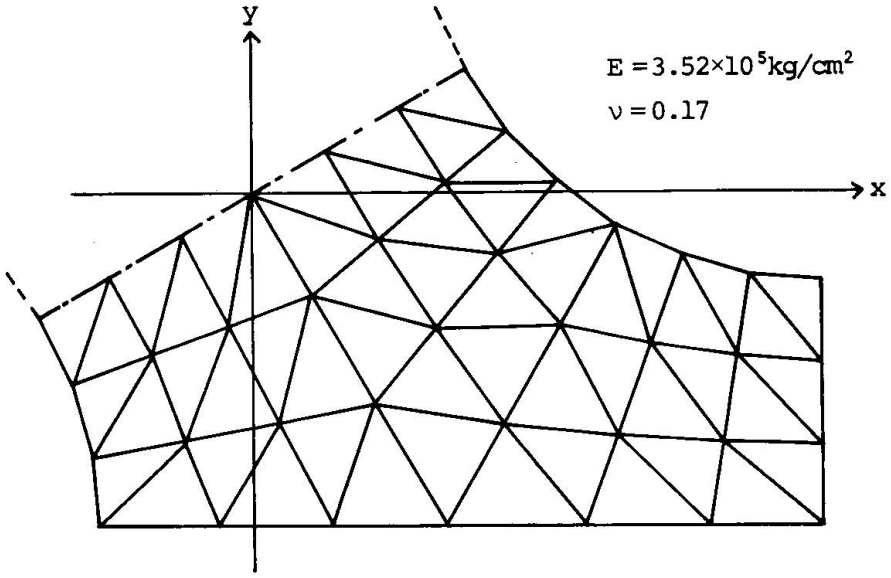

(a) Mesh Division (Plain Strain Problem)

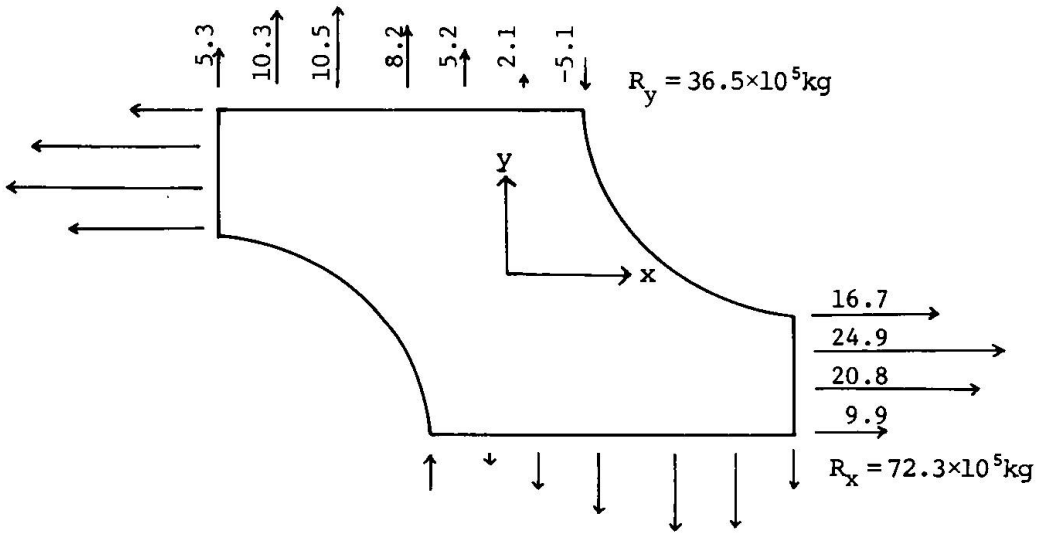

(b) Reactions for Prescribed Displacement $\delta_x = 83$cm

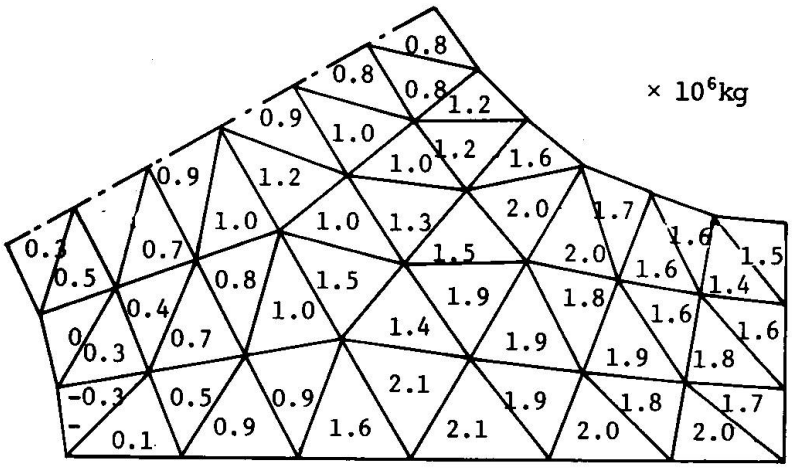

(c) Stress Resultants in z-Direction

Fig.5 Plain Strain Analysis of Unit Area for d_1, d_2 and d_3

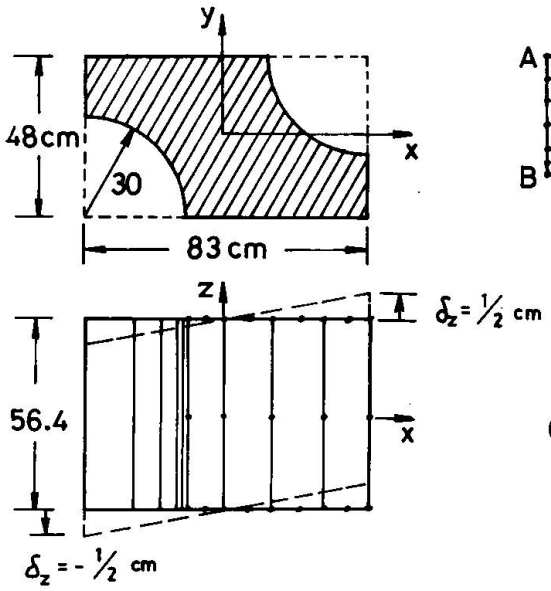

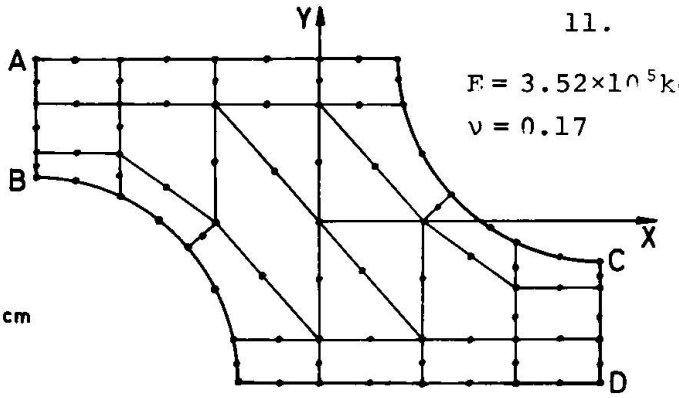

(a) Prescribed Displacements and Idealization by Iso-Parametric Elements

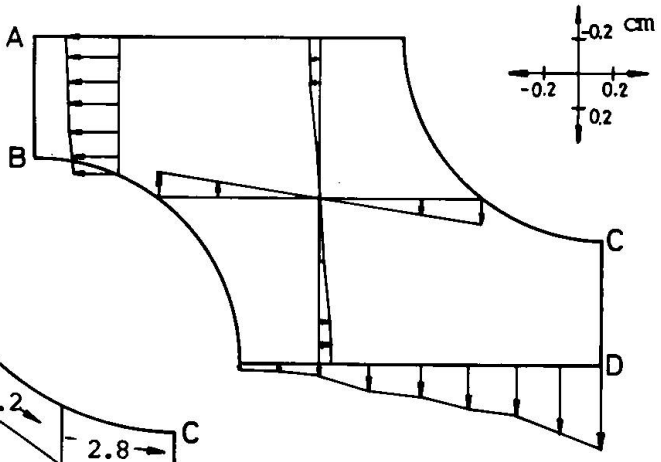

(b) Distribution of Vertical Displacement

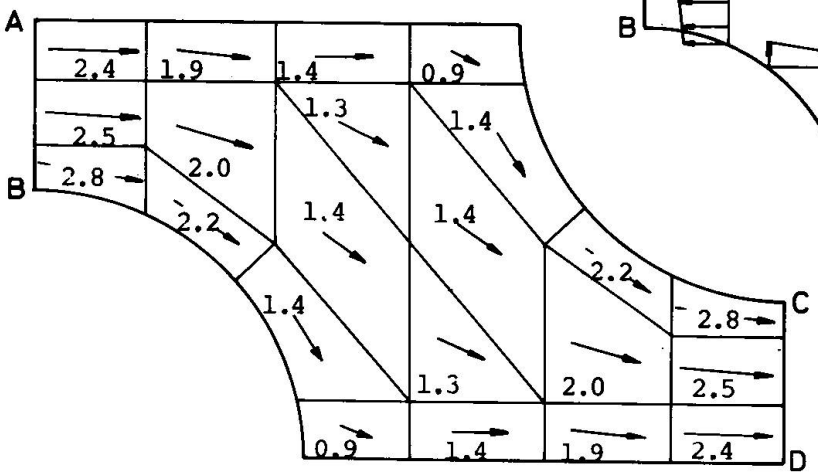

(c) Resultant of τ_{xz} and τ_{yz} figures : ratio to mean stress $\bar{\tau}_{xz}$

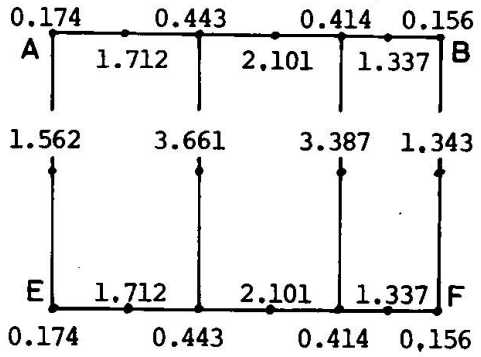

(d) Vertical Modal Reactions, $\times 10^6$kg

Fig.6 Shearing Stress Analysis of Unit Solid for d_5

As indicated in this example, the finite element analysis of the unit area enables consistent assessment of the equivalent elastic coefficients for the perforated solids with regular hole pattern. It must be also noted as one of the advantages of this method that it provides the factors of stress concentration relative to the mean stress intensity which will be obtained from the analysis of the transformed homogeneous field. The effect of the steel liner or reinforcement arround the holes to the effective stiffness can be allowed for by incorporating the corresponding elements in the finite element analysis.

3. METHOD OF SLICED SUBSTRUCTURES

In this section "the method of sliced substructures", a new method of simplified three-dimensional elastic analysis for podded boiler type PCPV, is proposed.

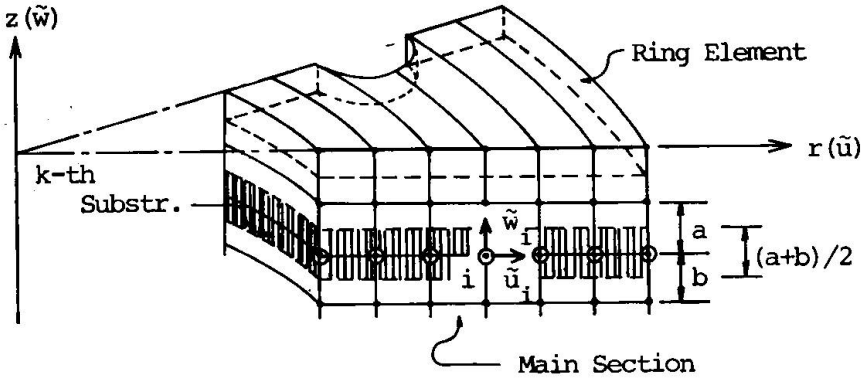

(a) Finite Element Mesh for Main Section

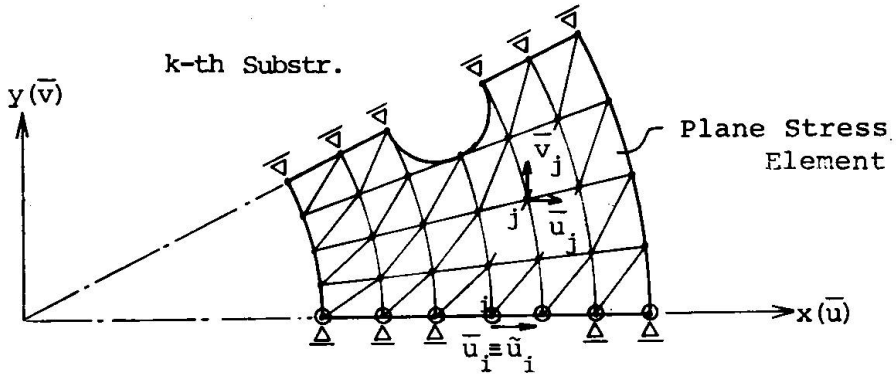

(b) Finite Element Mesh for Sliced Substructure

Fig. 7 Dual System of Idealization

1) Dual System of Finite Element Idealization

Let the vertical plane of symmetry located between two boiler pods be called the main section.

Let us idealize the solid portion to be analysed as the combination of two different kinds of finite element mesh.

The one system of the idealization is to divide the main section into a rectangular lattice pattern as shown in Fig.7(a), and to assign two-dimensional degrees of freedom, $\tilde{u}_i$ and $\tilde{w}_i$, to each nodes. This is the same practice as in the axi-symmetric analysis and the solid is represented as an assemblies of ring elements. It must be noted that the arc length of some ring elements is reduced from normal arc length by the existence of the opening for boiler.

As another system of the idealization, the solid is divided into layers of horizontal slices. As shown in Fig.7(a), the boundaries of the sliced layers are situated at the middle height of each lattice of the mesh for the main section. Therefore the thickness of the slice becomes $h=(a+b)/2$, where a and b represent the height of the upper and the lower lattice, respectively. The reference surface of the sliced layer is the horizontal plane on the end of which the nodes of the main section are resting.

Each sliced layer is now subdivided into a two dimensional mesh in the horizontal plane as shown in Fig.7(b). To each node of this mesh freedom of displacements $\bar{u}_j$ and $\bar{v}_j$, in x- and y-direction respectively, is assigned. It must be noted that displacement $\bar{u}_i$ of the node on one edge of the slice, which is the only component of displacement as the result of the condition of symmetry, is identical with the displacement $\tilde{u}_i$ assigned for the node of the main section.

2) Stiffness Matrix for Axial and Shearing Resistances

For the evaluation of the element stiffness based on the normal resistance in z-direction and the shearing resistance in r-z plane, we assume the displacement of axi-symmetric distribution

$$\tilde{u} = \tilde{u}(r, z)$$
$$\tilde{v} = \tilde{v}(r, z) \qquad (19)$$

which is shown in Fig.8. From this displacement field, the axi-symmetric distribution of strain is resulted as shown in Fig.8.

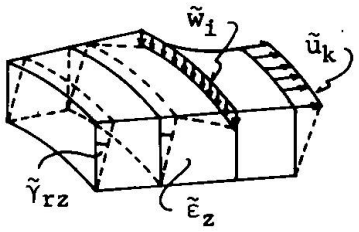

Fig.8 Distribution of Axi-symmetric Displacement and Strain

The important point is that, in evaluating the element stiffness, stress components σ_r and σ_θ caused by ε_r and ε_θ are not taken into account, because these components of resistance are supplemented later in the form of the stiffness of the sliced layers.

Thus, the element stiffness matrix is obtained by the formula

$$[\tilde{K}_e] = \int_{vol} [B]^T [\tilde{D}_1] [B] \, dV \qquad (20)$$

where [B] is strain matrix, $[\tilde{D}_1]$ is modified elasticity matrix, both for the axi-symmetric problem.

This formulation is basically the same to the element stiffness matrix of the axi-symmetric problem excepting the following two points.

i) In order to exclude the contribution of the resistance in r-θ plane, we use the elasticity matrix $[\tilde{D}_1]$ of the following form:

$$\{\tilde{\sigma}\} = [\tilde{D}_1] \{\tilde{\varepsilon}\} \qquad (21\text{-a})$$

$$\begin{Bmatrix} \tilde{\sigma}_r \\ \tilde{\sigma}_\theta \\ \tilde{\sigma}_z \\ \tilde{\tau}_{rz} \end{Bmatrix} = \begin{bmatrix} 0 & 0 & d_{13} & 0 \\ 0 & 0 & d_{23} & 0 \\ d_{31} & d_{32} & d_{33} & 0 \\ 0 & 0 & 0 & d_{44} \end{bmatrix} \begin{Bmatrix} \tilde{\varepsilon}_r \\ \tilde{\varepsilon}_\theta \\ \tilde{\varepsilon}_z \\ \tilde{\gamma}_{rz} \end{Bmatrix} \qquad (21\text{-b})$$

Eq.(21-b) means that we suppress the four coefficients in the ordinary [D] matrix for the axi-symmetric problem, and

ii) For the ring elements which cross the opening for boiler, the integration is carried out with regard to the actual volume reduced by the opening.

3) Stiffness Matrix for Sliced Substructures

The sliced layers are a kind of substructures which represents the partial components of the structural resistance, i.e. the resistance in the horizontal plane. The resistance of these substructures is to be combined with the axial and shearing resistances to form a total stiffness written in terms of the nodal freedom of the main section.

To each sliced substructure, two-dimensional degrees of freedom were assigned, that is we assumed the distribution of u and w which is constant within the thickness of the slice as shown in Fig.9. This means that the assumed distribution for the sliced substructures contains discontinuity in the boundaries of layers.

For each sliced substructure, the following stiffness ralation is formulated:

$$[\bar{K}] \{\bar{d}\} = \{f_s\} \qquad (22)$$

where $\{\bar{d}\}$: two-dimensional nodal displacements for the whole area of a sliced substructure

$\{f_s\}$: external forces in x and y directions applied to the nodes in a sliced substructure

$[\bar{K}]$: system stiffness matrix for plane stress problem of a sliced substructure

It must be noted that the stiffness matrix $[\bar{K}]$ in Eq.(22) is not the one for plane strain but that of plane stress. The reason can be explained by the fact that the constraint forces existing in plane strain state was already taken into account in the stiffness of the axi-symmetric resistance by taking the coefficients d_{13}, d_{23}, d_{31} and d_{32} in Eq.(21-b), and stiffness based on the plane stress state is to be su-perimposed.

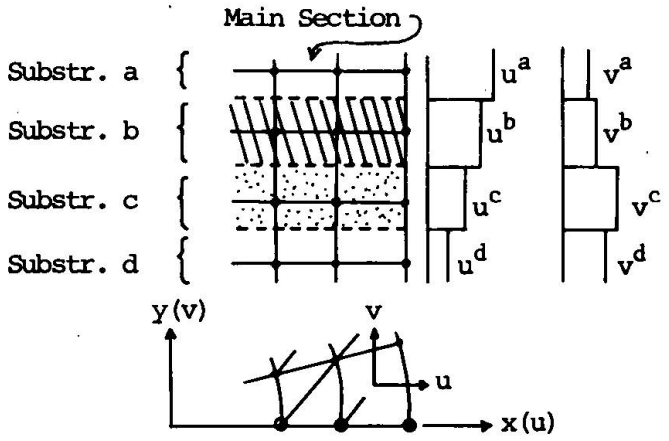

Fig.9 Assumed Distribution of Displacement for Sliced Substructures

Now, let us divide the nodal degrees of freedom of sliced substructure into two groups as shown in Fig.10, namely $\{\bar{u}_I\}$, a group of the radial displacements of the nodes resting on the main section and $\{\bar{d}_{II}\}$, a group of displacement components of all the other nodes.

In order to eliminate the freedom $\{\bar{d}_{II}\}$, Eq.(22) is rearranged into the following form:

$$\left[\begin{array}{c|c} \bar{K}_{11} & \bar{K}_{12} \\ \hline \bar{K}_{21} & \bar{K}_{22} \end{array}\right] \left\{\begin{array}{c} \bar{u}_I \\ \hline \bar{d}_{II} \end{array}\right\} = \left\{\begin{array}{c} f_{sI} \\ \hline f_{sII} \end{array}\right\} \qquad (23)$$

where

u_I : radial displacement of the nodes on the main section
: all the other nodal degrees of freedom
f_{sI} : external force of the nodes on the main section
f_{sII} : external force of the other nodes

The well-known procedure of the static condensation leads to the stiffness relation with regard to the retained freedom $\{\bar{u}_I\}$ as follows:

$$[\bar{K}_I]\{\bar{u}_I\} = \{\bar{f}_I\} \qquad (24\text{-a})$$

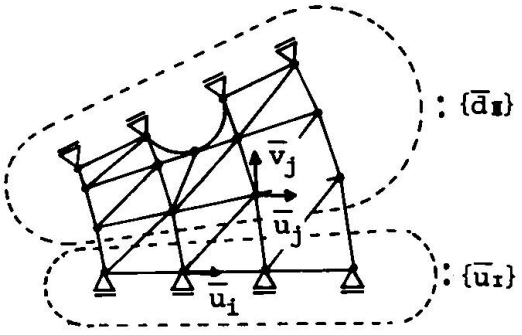

Fig. 10 Retained and Eliminated Displacements in Static Condensation

where $$[\bar{K}_I] = [\bar{K}_{11}] - [\bar{K}_{12}][K_{22}]^{-1}[\bar{K}_{21}] \qquad (24\text{-b})$$

: condensed stiffness matrix for $\{\bar{u}_I\}$

$$\{\bar{f}_I\} = \{f_I\} - [K_{12}][K_{22}]^{-1}\{f_{II}\} \qquad (24\text{-c})$$

: reduced external force corresponding to $\{\bar{u}_I\}$

The dimension of $[\bar{K}_I]$ matrix is $(m \times m)$, where m is twice the number of nodes contained in one horizontal line of the mesh of the main section.

4) Final Equation of Equilibrium

Basing on the fact that the retained degrees of freedom $\{\bar{u}_1\}$ of each sliced substructure are identical with the radial components of the nodal displacements $\{\tilde{d}\}$ of the main section, the final equilibrium equation with regard to the nodes in the main section can be composed by the superposition of the both stiffness relation derived in the above.

The composition of the final equation can be indicated by the following form:

$$\{[\tilde{K}]+[\bar{K}]\}\{\tilde{d}\} = \{\tilde{f}\}+\{\bar{f}\} \qquad (25)$$

where
- $\{\tilde{d}\}$: two-dimensional nodal degrees of freedom of the main section
- $\{\tilde{f}\}$: nodal external force in z-direction evaluated for the total arc length of the ring element
- $\{\bar{f}\}$: nodal external force in r-direction reduced from distributed external force on sliced substructure ,c.f. Eq.(24-c)
- $[\tilde{K}]$: stiffness matrix representing the axi-symmetric system of resistance
- $[\bar{K}]$: stiffness matrix representing the resistance in the horizontal plane derived from sliced substructures

In the final equation, the system stiffness matrix $[\tilde{K}]$ composed from the element stiffness matrix given in Eq.(20) has the same dimension and band structure as in the ordinary axi-symmetric problem of the given idealization of the main section. While, matrix $[\bar{K}]$ of the system stiffness matrix is composed of the condensed stiffness matrices $[\bar{K}_I]$ given in Eq.(24-b) for each substructure by placing them diagonally.

The composition of $[\bar{K}]$ matrix can be illustrated with respect to a simple layout of the main section and the slices shown in Fig.11. For this model, when we put $\{\tilde{d}\}$ vector as

$$\{\tilde{d}\} = \{\tilde{u}_1 \ \tilde{w}_1 \ \tilde{u}_2 \ \tilde{w}_2 \ \tilde{u}_3 \ \cdots\cdots\} \tag{26}$$

$[\bar{K}]$ matrix and load vectors take the following form:

$$[\bar{K}] = \begin{array}{c} \begin{array}{ccc} \tilde{d}_{1\sim4} & \tilde{d}_{5\sim8} & \tilde{d}_{9\sim12} \end{array} \\ \left[\begin{array}{c|c|c} \bar{K}^a & & \\ \hline & \bar{K}^b & \\ \hline & & \bar{K}^c \end{array}\right] \end{array} \tag{27-a}$$

where

$$[\bar{K}^a] = \begin{array}{c} \begin{array}{cccccccc} \tilde{u}_1 & \tilde{w}_1 & \tilde{u}_2 & \tilde{w}_2 & \tilde{u}_3 & \tilde{w}_3 & \tilde{u}_4 & \tilde{w}_4 \end{array} \\ \left[\begin{array}{cc|cc|cc|cc} * & 0 & * & 0 & * & 0 & * & 0 \\ 0 & 0 & 0 & 0 & 0 & 0 & 0 & 0 \\ \hline * & 0 & * & 0 & * & 0 & * & 0 \\ 0 & 0 & 0 & 0 & 0 & 0 & 0 & 0 \\ \hline * & 0 & * & 0 & * & 0 & * & 0 \\ 0 & 0 & 0 & 0 & 0 & 0 & 0 & 0 \\ \hline * & 0 & * & 0 & * & 0 & * & 0 \\ 0 & 0 & 0 & 0 & 0 & 0 & 0 & 0 \end{array}\right] \end{array} \tag{27-b}$$

* : non-zero element

and

$$\tilde{f} = \{0 \ f_{z1} | 0 \ f_{z2} | 0 \ f_{z3} | \cdots\cdots | 0 \ f_{z12}\} \tag{28}$$

$$\bar{f} = \{\bar{f}_1^a \ 0 | \bar{f}_2^a \ 0 | \bar{f}_3^a \ 0 | \bar{f}_4^a \ 0 | \bar{f}_5^b \ 0 | \bar{f}_6^b \ 0 | \cdots\cdots | \bar{f}_8^b \ 0 | \bar{f}_9^c \ 0 | \cdots\cdots | \bar{f}_{12}^c \ 0\} \tag{29}$$

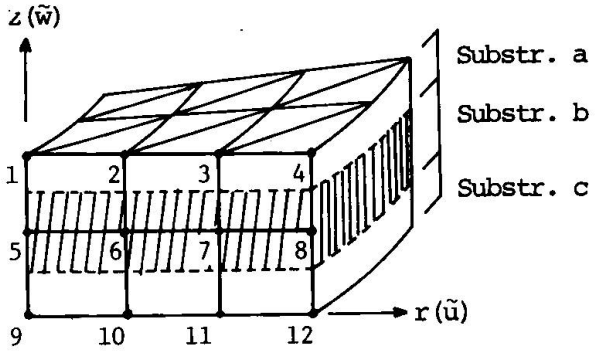

Fig. 11 Example of Layout of Main Section and Substructures

5) Evaluation of Stresses

The nodal displacements of the main section $\{\tilde{d}\}$, being substituted back into $\{\bar{u}_I\}$ in Eq.(23), yields the nodal displacement of the substructures. In evaluating the stress in the elements of each slice, the effect of Pisson's ratio i.e. σ_x and σ_y caused by $\tilde{\varepsilon}_z$ must be superimposed to the plane stress. Thus the final form of the stress of the slices is given as follows:

$$\{\sigma_e\} = \{\tilde{\sigma}(\tilde{\varepsilon}_z)\} + \{\bar{\sigma}\} \tag{30-a}$$

where $$\{\bar{\sigma}\} = \{\bar{\sigma}_x \ \bar{\sigma}_y \ \bar{\tau}_{xy}\} : \tag{30-b}$$

stress of an element of sliced substructure obtained by using stress matrix for plane stress problem

$$\{\tilde{\sigma}(\tilde{\varepsilon}_z)\} = \begin{Bmatrix} \tilde{\sigma}_x \\ \tilde{\sigma}_y \\ 0 \end{Bmatrix} = \begin{bmatrix} E_{13} \\ E_{23} \\ 0 \end{bmatrix} \tilde{\varepsilon}_z : \tag{30-c}$$

stress induced by $\tilde{\varepsilon}_z$ of the ring elements

It must be noted that, in Eqs.(30), $\{\bar{\sigma}\}$ is calculated with respect to the each element of the substructures while $\{\tilde{\sigma}(\tilde{\varepsilon}_z)\}$ is calculated with respect to the each ring element of the main section, both being to be superimposed according to the geometrical co-relation.

4. EXAMPLES OF ANALYSIS BY THE METHOD OF SLICED SUBSTRUCTURES

In order to illustrate the application of the method of sliced substructures and to show its validity and efficiency, the following two simple problems were analysed.

Example 1: Analysis of a Thick-Walled Cylinder without Hole

Thick-walled cylinder partially subjected to inner pressure, shown in Fig.12(a), was analyzed using both of the ordinaly axi-symmetric and sliced substructure methods. As the problem is purely axi-symmetric the method of sliced substructure must lead to the same result to that of the axi-symmetric analysis. Finite element idealization shown in Fig.12(b) was used.

Figs.12(c) and (d) shows the comparison of the both analyses with regard to displacement and stress distribution, respectively, of the main section. It can be seen that almost identical results were obtained from both method.

Table I indicates the comparison of computing time for axi-symmetric and sliced substructure analyses.

	Axi-Symmetric	Sliced Substructures
Data Input and Stiffness Matrix	3.3 sec.	38.4 sec.*
Solving Eq.	2.3	4.0
Back Substitution and Out Put	1.5	4.6
Total	7.1 sec.	47.0 sec.

* including 24.0 sec. of matrix inversion for a substructure

Table I Computing Time for Example 1, IBM 360/195

Example 2: Analysis of a Thick-Walled Cylinder with Holes

A thick-walled cylinder of the same dimensions and loading as Example 1 but having vertical holes like boiler pods was analyzed. The problem is three-dimensional in this case and the solution obtained by the method of sliced substructures was compared with that of the ordinary three-dimensional analysis by the use of iso-parametric elements.

Fig.13(a) shows the definition of the problem. The finite element idealization used in both method is shown in Fig.13(b).

The comparison between the results from both method is presented in Figs.13(c) and (d).

CONCLUSIONS

In this paper a simplified method of elastic analysis for podded boiler type PCPV was presented.

A finite element analyses of the unit area of the hole pattern enable consistent method of evaluating the coefficients of elasticity of the transversely isotropic body equivalent to the stand pipe zone of top slab.

Also, a newly developed "method of sliced substructures" enables us to analyze the three-dimensional problems of PCPV within the same degrees of freedom as the axi-symmetric problems, where the disturbance of stress by the boiler pods is fully allowed for.

For the problems of the same scale experienced in the examples, the ratio of necessary computing time of axi-symmetric / sliced substructures/ was 7 / 47 , respectively. The computing time for the method of substructure can be further reduced by introducing the iso-parametric two-dimensional elements in the idealization of the sliced substructures, because a large part of the total computing time was occupied by the matrix inversion contained in the static condensation of the substructures.

ACKNOWLEDGEMENTS

The sincere appreciation is expressed to Dr. Y. Hangai, University of Tokyo; Mr. S. Shioya, Nihon University; Mr. Y. Isobata, Mr. N. Tanaka and Mr. H. Akiyama, Shimizu Construction Co. Ltd. to whom the author greatly indepted for their collaboration in all phases of this research.

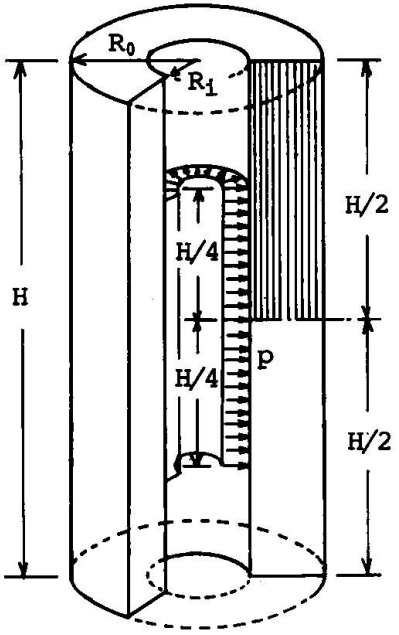

$R_0 = 15.0\,m$, $R_i = 6.0\,m$

$H = 60.0\,m$

$p = 45 kg/cm^2$

$E = 3.0 \times 10^5 kg/cm^2$

$\nu = 0.17$

(a) Analyzed Model

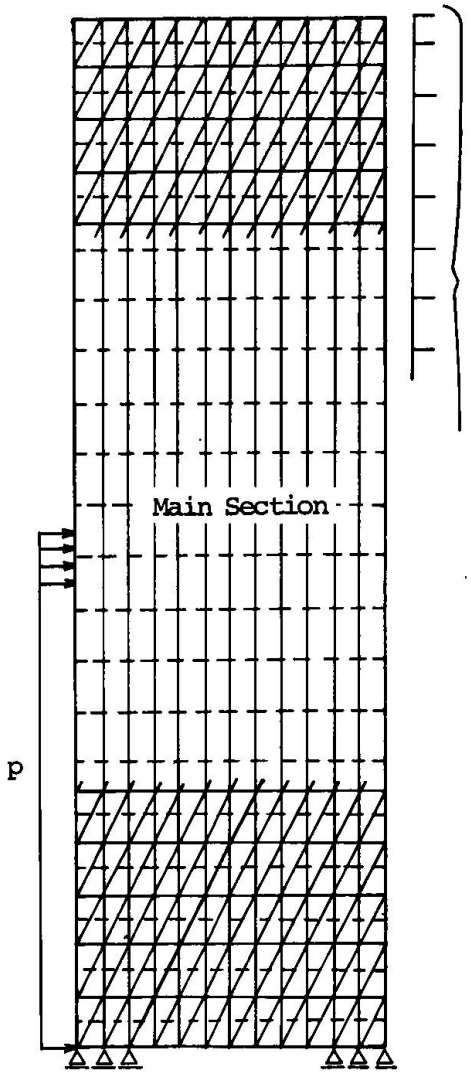

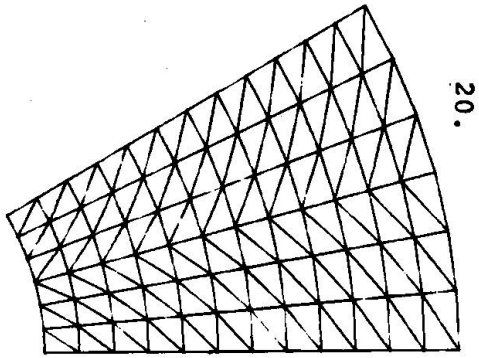

Sliced Substructure

Main Section : 480 elements
273 nodes
21 slices
Each Slice : 144 elements
91 nodes

(b) Finite Element Idealization

Fig. 12 Analysis of a Thick-Walled Cylinder Partially Loaded by Inner Pressure

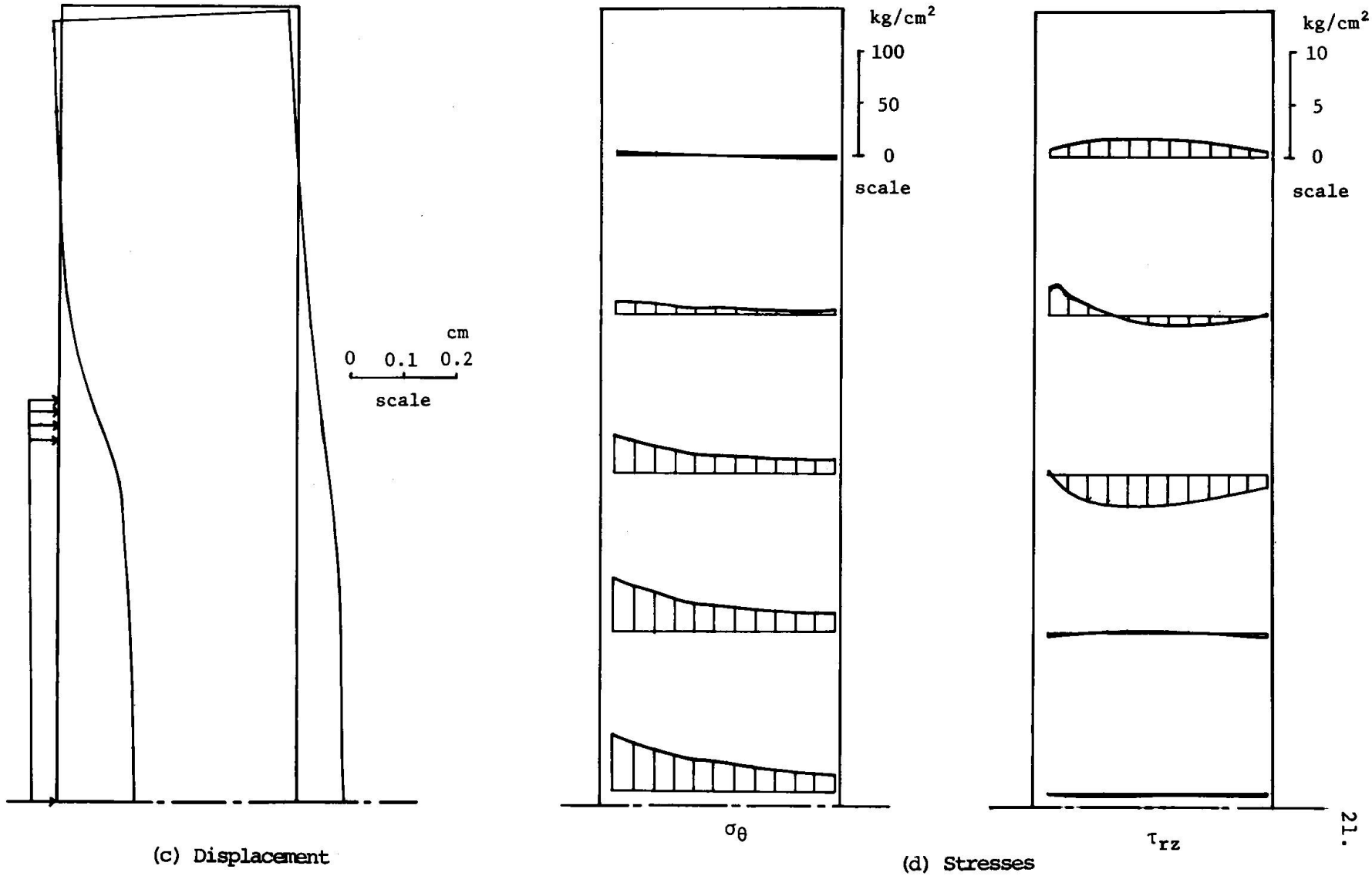

(c) Displacement

(d) Stresses

Fig 12 Analysis of a Thick-Walled Cylinder Partially Loaded by Inner Pressure
(Difference of results from both methods is invisible in the diagrams)

R_o = 15.0 m
R_i = 6.0 m
H = 60.0 m
D = 4.5 m
p = 45.0 kg/cm^2
E = 3.0 × 10^{5}kg/cm^2
ν = 0.17

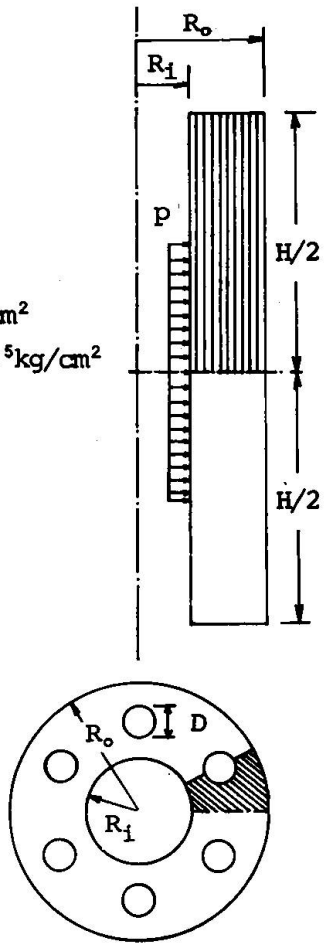

(a) Analyzed Model

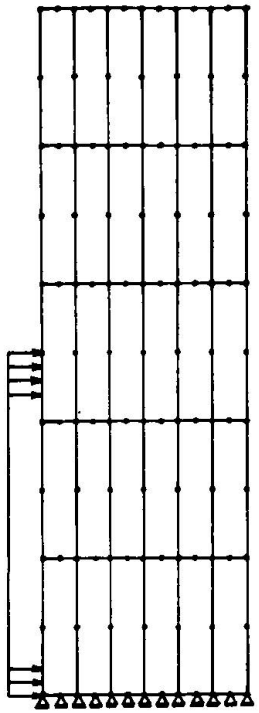

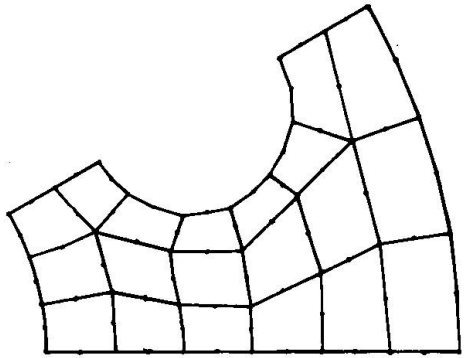

Three Dimensional Analysis

100 iso-parametric elements

658 nodes

Sliced Substructure Analysis

Mesh of Main Section:

the same as Fig.11(b)

Idealization of each

Sliced Substructure:

160 elements

103 nodes

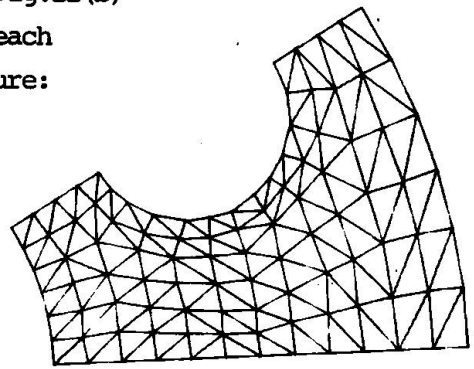

(b) Finite Element Idealization

Fig.13 Analysis of Thick-Walled Cylinder with Holes

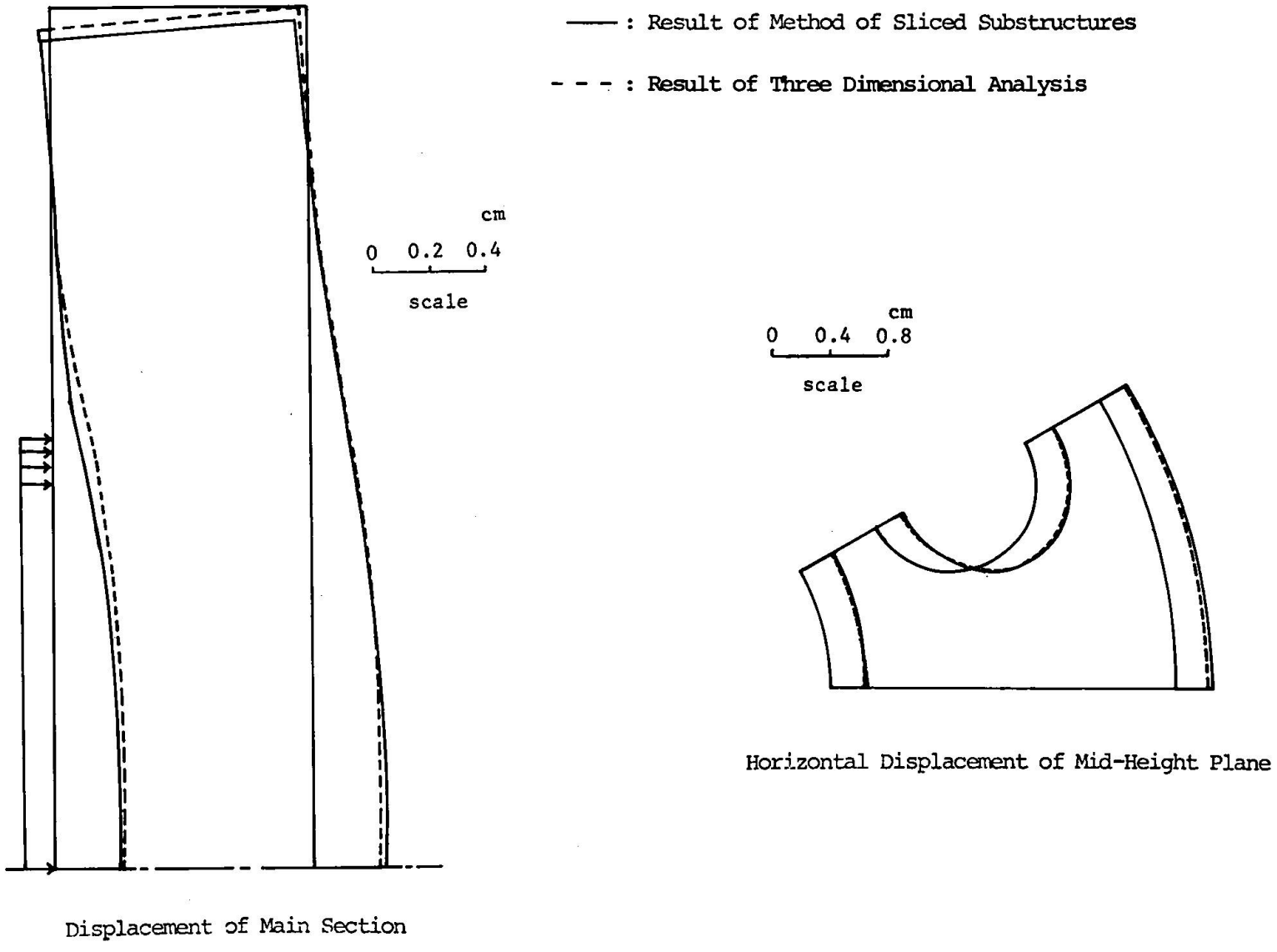

(c) Distribution of Displacement

Fig. 13 Analysis of Thick-Walled Cylinder with Holes

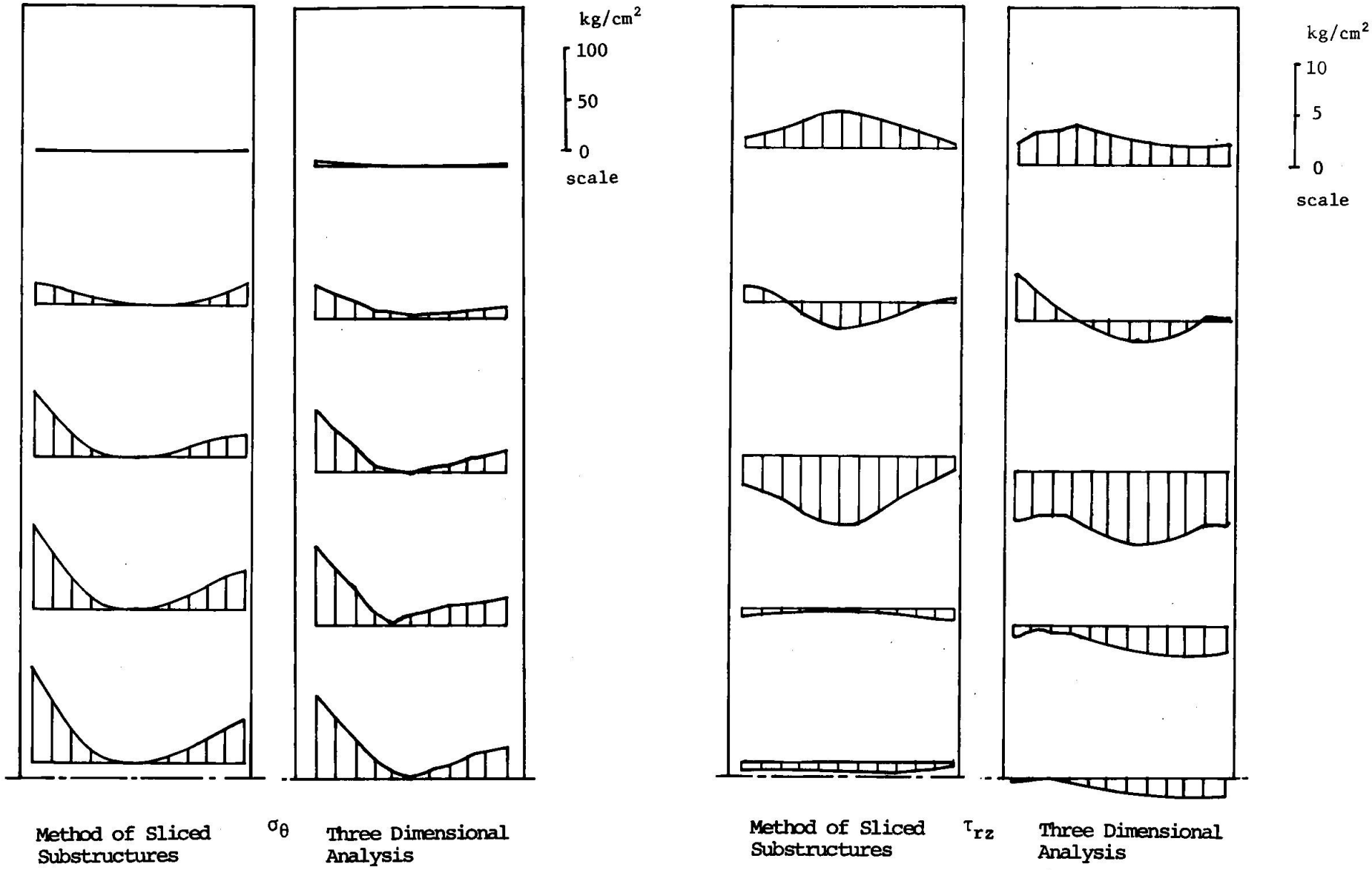

(d) Stress Distribution

Fig. 13 Analysis of Thick-Walled Cylinder with Holes

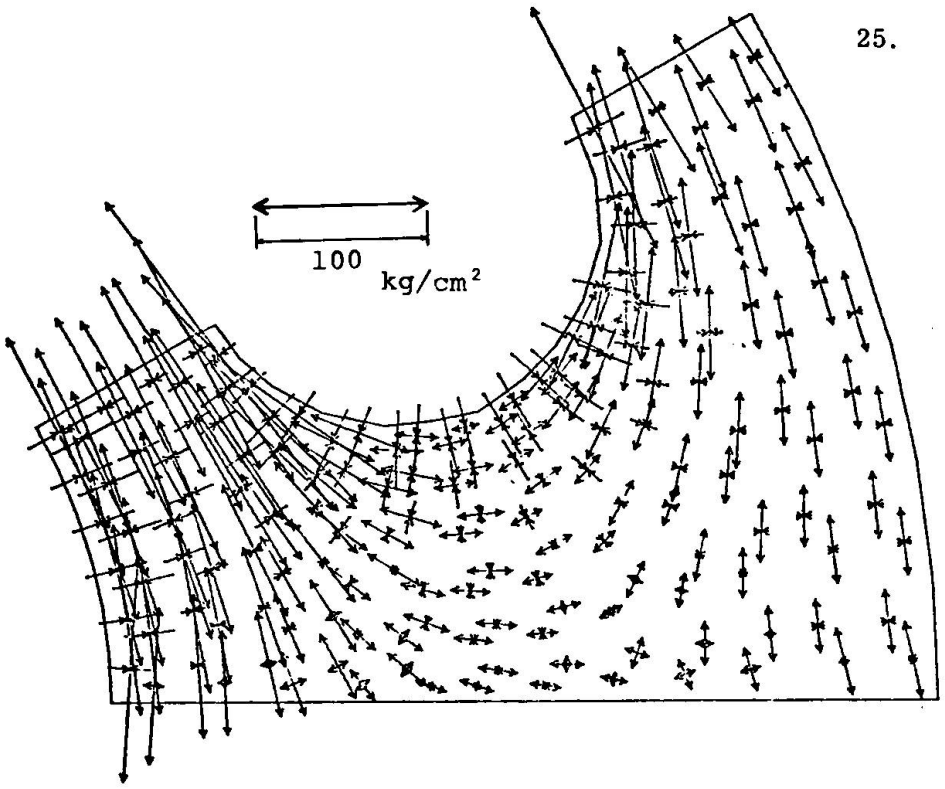

Result by Method of Sliced Substructures

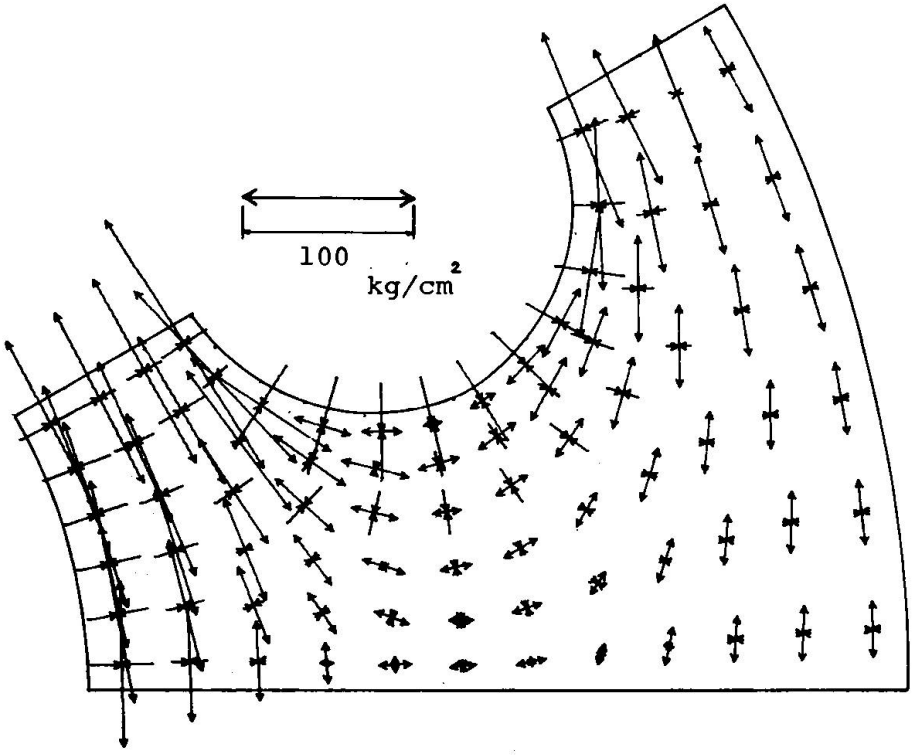

Result by Three Dimensional Analysis

(d) Principal Stress Distribution

Fig. 13 Analysis of Thick-Walled Cylinder with Holes

REFERENSES

[1] J.H.Argyris, K,E.Buck, D,W.Scharpf and K.J.Willam, "Linear Methods of Structural Analysis", 1st SMIRT Conference, Berlin, 1971; Nuclear Engineering and Design, Vol.19, 1972, pp.139-167.

[2] R.W.Bailey and R.Fidler, "Stress Analysis of Plates and Shells Containing Patterns of Reinforced Holes", Nuclear Engineering and Design, Vol.3, 1966, pp.41-53.

[3] H.M.S. Abdul-Wahab and J.Harrop, "The Rigidity of Perforated Plates with Reinforced Holes", Nuclear Engineering and Design, Vol. 5, 1967, pp.134-141.

[4] D.J.Lewis, J,Irving and G,D,T.Carmichael, "Advances in the Analysis of Prestressed Concrete Pressure Vessels", 1st SMIRT Conference, 1971; Nuclear Engineering and Design, Vol.20, 1972, pp.543-573.

[5] Y.R.Rashid and W.Rockenhauser, "Pressure Vessel Analysis by Finite Element Techniques", Proc. Conf.on PCPV, London, 1967, Inst. Civil Engrs., 1968, pp.375-383.

[6] O.C.Zienkiewicz, B.M.Irons, J,Ergatoudis, S.Ahmad and F.C.Scott, "Iso-Parametric and Associated Element Families for Two-and Three-Dimensional Analysis", Finite Element Methods in Stress Analysis, ed. I.Holand and K,Bell, TAPIR, Trondheim, 1969, pp.383-432.

[7] O.C,Zienkiewicz, D.R.J.Owen, D.V.Phillips and G.C.Nayak, "Finite Element Methods in the Analysis of Reactor Vessels", 1st SMIRT Conference, Berlin, 1971; Nuclear Engineering and Design, Vol.20, 1972, pp.507-541.

[8] P.Meijers, "Three-dimensional Stress Analysis for Perforated Plates with a Regular Triangular Hole Pattern", Inst. TNO for Mechanical Construction, Delft, Rep. No.81290, 1971.

[9] P.Meijers, "Review of ASKA Program", Numerical and Computer Methods in Structural Mechanics, Proc. Conf., Urbana, 1971, ed. S,J.Fenves, N.Perone, A,R.Robinson and W.C.Schnobrich, Academic Press, 1973, pp.123-149.

[10] Y.Tsuboi, S.Kawamata, N,Tanaka, "Finite Element Analysis of Continua —— Effective Rigidity of Perforated Body, Proc. Annual Convention, Architectural Institution of Japan, Oct. 1967

[11] F,Kikuchi, "An Example of Partial Approximation in the Finite Element Method, Proc. 23rd Japan Nat. Congr. Theo. Appl. Mech, 1973, to be published.

[12] F.Kikuchi, "On the Validity of an Approximation Available in Finite Element Shell Analysis, to appear, 1974.

[13] F.Kikuchi, "Theory and Example of Partial Approximation in the Finite Element Method, to appear, 1974.

[14] A.E.Green and W.Zerna, "Theoretical Elasticity", Oxford at the Clarendon Press, 1960, p.159.

[15] S.G.Lekhnitskii, "Theory of Elasticity of an Anisotropic Elastic Body", Holden-Day, 1963.

[16] O,C,Zienkiewicz and Y,K,Cheung, "The Finite Element Method in Structural and Continuum Mechanics", McGraw-Hill, 1967, p.50.

RESUME

On discute une méthode simplifiée pour l' analyse élastique tridimensionnelle par éléments finis d' un caisson en béton précontraint du type "Podded Boiler".

La première partie traite une méthode pour l' évaluation de la rigidité efficace de la zone avec pénétrations, où l' on utilise des analyses tridimensionnelles par éléments finis de la surface unitaire de un système régulier de trous.

Dans la deuxième partie on propose la nouvelle méthode des sous-structures coupées pour l' analyse tridimensionnelle simplifiée des caissons.

La rigidité du caisson vient déterminée comme combinaison de la matrice de problèmes axial-simmétriques modifiés et des matrices de rigidité bidimensionnelles de sous-structures coupées horizontalement. La méthode permet l' analyse tridimensionnelle des problèmes de caissons en tenant compte de l' effet des "Boiler Pods", et en maintenant les mêmes degrés de liberté que dans l' analyse axial-simmétrique.

La validité de la méthode est prouvée par des exemples numériques.

ZUSAMMENFASSUNG

Im ersten Teil wird ein Verfahren beschrieben, das es erlaubt die effektive Festigkeit von perforierten Zonen zu bewerten mit Hilfe von Analysen mit endlichen Elementen einer Einheitsfläche von regelmässigen Perforationssystemen.

Im zweiten Teil wird eine neue vereinfachte Methode für tridimensionale Analysen von Spannbeton-Druckbehältern, die sogenannte "Sliced-Structures Method" erklärt. Die Steifigkeitsberechnung für diese Behälter ist eine Kombination der Festigkeitsmatrix von modifizierten axialsymmetrischen Problemen und der zweidimensionalen Festigkeitsmatrix von Querschnitten von Unterkonstruktionen; bei der Berücksichtigung des "Boiler Pod" Effekts ist der selbe Grad von Freiheit gestattet wie bei der axialsymmetrischen Analyse. Die Gültigkeit der neuen Methode wird mit einigen Zahlenbeispielen belegt.

Leere Seite
Blank page
Page vide